

# Efficiency bounds for bipartite information-thermodynamic systems

Shihao Xia<sup>1</sup>, Shuanglong Han<sup>1</sup>, Ousi Pan<sup>1</sup>, Yuzhuo Pan<sup>2</sup>, Jincan Chen<sup>1</sup>, and Shanhe Su<sup>1\*</sup>

<sup>1</sup>*Department of Physics, Xiamen University, Xiamen 361005, People's Republic of China*

<sup>2</sup>*College of Physics and Information Engineering,  
Quanzhou Normal University, 362000, People's Republic of China*

(Dated: July 4, 2024)

This study introduces a novel approach to derive a lower bound for the entropy production rate of a subsystem by utilizing the Cauchy-Schwarz inequality. It extends to establishing comprehensive upper and lower bounds for the efficiency of two subsystems. These bounds are applicable to a wide range of Markovian stochastic processes, which enhances the accuracy in depicting the range of energy conversion efficiency between subsystems. Empirical validation is conducted using a two-quantum-dot system model, which serves to confirm the effectiveness of our inequality in refining the boundaries of efficiency.

## I. INTRODUCTION

Over the past two decades, the field of stochastic thermodynamics has witnessed remarkable progress, greatly enriching our comprehension of physical phenomena occurring in small fluctuating systems. This framework has unveiled the inherent connection between thermodynamic irreversibility and non-equilibrium fluctuations.

Simultaneously, the study of stochastic thermodynamics has facilitated explorations into the interrelationship between information and thermodynamics, as well as the thermodynamic limits of fluctuating mesoscopic systems. [1, 2]. A pivotal discovery in this domain is Landauer's principle [3], which quantifies the heat dissipation required for the erasure of information in the limit of slow quasi-static processes [4]. This principle has been empirically validated in both classical and quantum frameworks [5–7]. In the era of high-speed computational demands, a noteworthy breakthrough has been the investigation of the energy consumption associated with finite-time information erasure [8–10]. Leveraging the unique synergy between information and thermodynamics, researchers have devised various heat engines, such as the Szilard engine [11–13] and molecular engines [14–16]. These advancements have opened up new avenues for the design of miniature heat engines.

On the other hand, thermodynamic inequalities have established foundational limits on entropy production and energy usage [16–18], deepening our understanding of thermodynamics and providing valuable insights into microsystems. A multitude of studies have corroborated the Clausius statement of the second law of thermodynamics by employing thermodynamic inequalities. This consensus and the substantial research interests in this field signify its importance and widespread relevance. [16, 19–31]. In the pursuit of establishing theoretical bounds, researchers have adopted various methodologies. Notably, Jensen bounds [15, 32] and Cramér-Rao [33] bounds represent significant approaches in delineating

these constraints.

While existing researches provide valuable insights into the boundaries of energy conversion and entropy production, our investigation adopts an alternative framework. Specifically, we leverage the Cauchy-Schwarz inequality [21, 22] within the stochastic thermodynamics context to derive a more refined lower bound for the entropy production rate in subsystems. This approach enables us to obtain an accurate approximation to the energy conversion efficiency of these subsystems.

The structure of this paper is organized as follows: Section II delves into the examination of stochastic thermodynamics in bipartite systems, where the efficiency bounds for subsystems are derived. Section III focuses on the double quantum dot system and derives expressions for the associated thermodynamic quantities by calculating the transition frequency. By building upon the double quantum dot model, section IV presents our findings in a detailed discussion. Finally, the paper concludes with section V, which summarizes the key insights gained from the study.

## II. STOCHASTIC THERMODYNAMICS OF BIPARTITE SYSTEMS

### A. Stochastic dynamics for a bipartite system

We adopt a conventional stochastic process model for a bipartite system  $Z$ , which is described thoroughly and extensively in [34]. The state of  $Z$  is described by  $z = (x, y)$  with  $x$  and  $y$  representing the particle counts in subsystems  $X$  and  $Y$ , respectively. The state  $z$ 's time-dependent probability,  $p(z)$ , evolves following the Markovian master equation

$$\dot{p}(z) = \sum_{z',v} J_{zz'}^v. \quad (1)$$

Here, the flux  $J_{zz'}^v = W_{zz'}^v p(z') - W_{z'z}^v p(z)$  hinges on the time-independent transition rate  $W_{zz'}^v$  from state  $z'$  to state  $z$  induced by reservoir  $v$ , and the reverse tran-

\* sushanhe@xmu.edu.cn

sition rate  $W_{z'z}^v$ . The transition rate matrix, being non-negative  $W_{zz'}^v \geq 0$  for  $z \neq z'$ , restricts the bipartite structure from allowing simultaneous state changes in both subsystems. Consequently, the form of  $W_{zz'}^v$  is constrained to

$$W_{zz'}^v = \begin{cases} W_{xx'|y}^v & (x \neq x', y = y') \\ W_{yy'|x}^v & (x = x', y \neq y') \\ 0, & (\text{otherwise}) \end{cases} \quad (2)$$

where  $W_{xx'|y}^v$  signifies the transition rate for subsystem  $X$  moving from state  $x'$  to state  $x$  given that subsystem  $Y$  is in state  $y$ , and similarly,  $W_{yy'|x}^v$  for transitions within subsystem  $Y$ .

### B. Information thermodynamics of the bipartite system

Due to the bipartite nature, the entropy production rate  $\dot{\sigma}$  of the bipartite system can be split into two components:

$$\dot{\sigma} = \dot{\sigma}^X + \dot{\sigma}^Y. \quad (3)$$

Herein,  $\dot{\sigma}^X$  and  $\dot{\sigma}^Y$  represent the partial entropy production rates resulting from transitions in  $X$  and  $Y$ , respectively, which are expressed as

$$\dot{\sigma}^X = \frac{1}{2} \sum_{x,x',y,v} J_{xx'|y}^v \ln \frac{p(x',y) W_{xx'|y}^v}{p(x,y) W_{x'|x}^v} \quad (4)$$

and

$$\dot{\sigma}^Y = \frac{1}{2} \sum_{y,y',x,v} J_{yy'|x}^v \ln \frac{p(y',x) W_{yy'|x}^v}{p(y,x) W_{y'|y}^v}. \quad (5)$$

The entropy flow towards the environment,  $\dot{S}_r$ , is given by:

$$\dot{S}_r = \dot{S}_r^X + \dot{S}_r^Y \quad (6)$$

where

$$\dot{S}_r^X = \frac{1}{2} \sum_{x,x',y,v} J_{xx'|y}^v \ln \frac{W_{xx'|y}^v}{W_{x'|x}^v} \quad (7)$$

and

$$\dot{S}_r^Y = \frac{1}{2} \sum_{y,y',x,v} J_{yy'|x}^v \ln \frac{W_{yy'|x}^v}{W_{y'|y}^v}, \quad (8)$$

correspond to the energy flux from  $X$  and  $Y$  to their respective environment.

$$\dot{I}^X = \frac{1}{2} \sum_{x,x',y,v} J_{xx'|y}^v \ln \frac{p(y|x)}{p(y|x')} \quad (9)$$

and

$$\dot{I}^Y = \frac{1}{2} \sum_{x,x',y,v} J_{yy'|x}^v \ln \frac{p(x|y)}{p(x|y')} \quad (10)$$

quantify how information exchanges between the two subsystems. When  $\dot{I}^X > 0$ , subsystem  $X$  is measuring  $Y$ ; vice versa,  $\dot{I}^X < 0$  signifies that  $X$  is consuming information in order to extract energy.

From Eq. (4) to Eq. (10), it is evident that  $\dot{\sigma}^X$  and  $\dot{\sigma}^Y$  must be non-negative, which can be split into three components as [35]:

$$\dot{\sigma}^X = \dot{S}_r^X + \dot{S}_r^{X'} - \dot{I}^X \geq 0 \quad (11)$$

$$\dot{\sigma}^Y = \dot{S}_r^Y + \dot{S}_r^{Y'} - \dot{I}^Y \geq 0. \quad (12)$$

Upon reaching a steady state, the system settles into a stationary probability distribution [ $\dot{p}(x) = 0$  and  $\dot{p}(y) = 0$ ], leading to  $\dot{S}_r^{X(Y)} = 0$ . Thus, Eqs. (11) and (12) are simplified as follows:

$$\dot{\sigma}^X = \dot{S}_r^X - \dot{I}^X \geq 0 \quad (13)$$

and

$$\dot{\sigma}^Y = \dot{S}_r^Y - \dot{I}^Y \geq 0. \quad (14)$$

In scenarios where  $\dot{I}^X > 0$ , as Eq. (13), the information  $\dot{I}^X$  is constrained by the entropy flow to the environment  $\dot{S}_r^X$ , which represents the dissipation required for  $X$  to learn about  $Y$ . Information then becomes a resource for energy extraction or work execution via feedback on  $Y$ .

### C. The thermodynamic efficiency of two subsystems

We now shift our focus to the nonequilibrium steady state, in which each subsystem exchanges work and heat with their respective external reservoirs. To articulate thermodynamic quantities, it's assumed that the transition rates adhere to the local detailed balance condition specified by the following equation[33, 36]

$$\ln \frac{W_{xx'|y}^v}{W_{x'x|y}^v} = \beta \left( \epsilon_{x'y} - \epsilon_{xy} + \Delta_{xx'|y}^v \right), \quad (15)$$

where  $\beta = (k_B T)^{-1}$  is the inverse temperature by assuming that all the reservoirs are at temperature  $T$ ,  $\epsilon_{xy}$  represents the energy of state  $(x, y)$ , and  $\Delta_{xx'}^y$  is the energy provided by an external agent during the transition  $(x', y) \rightarrow (x, y)$ . The parameter  $\Delta_{xx'}^y$  will affect the heat flow. For the quantum dot system interacting with an electron reservoir,  $-\Delta_{xx'}^y$  represents the chemical potential of the reservoir, which will be further illustrated in Sec. III. The average rate of heat absorbed by  $X$  from the environment is then determined by

$$\dot{Q}^X = -\frac{k_B T}{2} \sum_{x, x', y, v} J_{xx'|y}^v \ln \frac{W_{xx'|y}^v}{W_{x'x|y}^v}. \quad (16)$$

The average rate of work done by the external agent on  $X$  is identified as

$$\dot{W}^X = \frac{1}{2} \sum_{x, x', y, v} J_{xx'|y}^v \Delta_{xx'|y}^v. \quad (17)$$

Subsequently, the average rate of change of internal energy, interpreted as the work done by  $X$  on  $Y$ , is expressed as

$$\dot{W}^{X \rightarrow Y} = \frac{1}{2} \sum_{x, x', y, v} J_{xx'|y}^v (\epsilon_{xy} - \epsilon_{x'y}). \quad (18)$$

The rates  $\dot{W}^Y$ ,  $\dot{Q}^Y$ , and  $\dot{W}^{Y \rightarrow X}$  are similarly defined for  $Y$ . Note that each subsystem adheres to the first law of thermodynamics that encapsulates local energy conservation:

$$\begin{aligned} \dot{W}^{X \rightarrow Y} &= \dot{W}^X + \dot{Q}^X, \\ \dot{W}^{Y \rightarrow X} &= \dot{W}^Y + \dot{Q}^Y. \end{aligned} \quad (19)$$

Furthermore, at steady state, the powers and information flows satisfy  $\dot{W}^{X \rightarrow Y} + \dot{W}^{Y \rightarrow X} = 0$  and  $\dot{I}^X + \dot{I}^Y = 0$ . On the basis of Eqs. (19), (13), and (14), each subsystem conforms to the second law of thermodynamics at the steady state:

$$\begin{aligned} \dot{\sigma}^X &= \beta \dot{W}^X - \beta \dot{W}^{X \rightarrow Y} - \dot{I}^X \geq 0, \\ \dot{\sigma}^Y &= \beta \dot{W}^Y - \beta \dot{W}^{Y \rightarrow X} - \dot{I}^Y \geq 0. \end{aligned} \quad (20)$$

Within this framework, each subsystem satisfies the first and second laws. Without loss of generality, let  $Y$  be the "upstream" subsystem, with the rate of work input to  $Y$  being positive, denoted as  $\dot{W}^Y > 0$ . We will limit our discussion to functional machines that produce work

from subsystem  $X$ , i.e.,  $\dot{W}^X \leq 0$ . They thus each have their own thermodynamic efficiencies:

$$\begin{aligned} \eta^Y &:= \frac{\beta \dot{W}^{X \rightarrow Y} + \dot{I}^Y}{\beta \dot{W}^Y}, \\ \eta^X &:= \frac{-\beta \dot{W}^X}{\beta \dot{W}^{Y \rightarrow X} + \dot{I}^Y}. \end{aligned} \quad (21)$$

As discussed in Ref. [15], the efficiency of subsystem  $Y$ , denoted as  $\eta^Y$ , reflects how effectively  $Y$  transforms the input work into free energy available for subsystem  $X$ . Conversely,  $\eta^X$  measures the efficiency of  $X$  in converting this free energy back into output work. The product of these efficiencies,  $\eta^Y \eta^X = -\dot{W}^X / \dot{W}^Y = \eta^T$ , defines the overall thermodynamic efficiency of the system. These efficiencies remain valid as long as both  $\dot{W}^Y$  and  $\beta \dot{W}^{Y \rightarrow X} + \dot{I}^Y$  are strictly positive. This ensures that the conditions  $0 \leq \eta^X \leq 1$  and  $0 \leq \eta^Y \leq 1$  are satisfied, as derived from Eq. (20).

#### D. Bounds on the efficiencies of two subsystems

Equation (20) yields dual equalities:

$$\dot{\sigma}^X - \beta \dot{W}^X = \beta \dot{W}^{Y \rightarrow X} + \dot{I}^Y = \beta \dot{W}^Y - \dot{\sigma}^Y. \quad (22)$$

Applying any lower bounds  $\dot{\sigma}_{LB}^X \leq \dot{\sigma}^X$  and  $\dot{\sigma}_{LB}^Y \leq \dot{\sigma}^Y$  to this equation facilitates the derivation of upper and lower bounds on  $\beta \dot{W}^{Y \rightarrow X} + \dot{I}^Y$ :

$$\dot{\sigma}_{LB}^X - \beta \dot{W}^X \leq \beta \dot{W}^{Y \rightarrow X} + \dot{I}^Y \leq \beta \dot{W}^Y - \dot{\sigma}_{LB}^Y. \quad (23)$$

Dividing Eq. (23) by  $\dot{W}^Y$  results in upper and lower bounds on the efficiency of  $Y$ :

$$\eta^T \left( 1 + \frac{\dot{\sigma}_{LB}^X}{-\beta \dot{W}^X} \right) \leq \eta^Y \leq 1 - \frac{\dot{\sigma}_{LB}^Y}{\beta \dot{W}^Y}. \quad (24)$$

Conversely, multiplying the reciprocal of Eq. (23) by  $-\dot{W}^X$  produces upper and lower bounds on the efficiency of  $X$ :

$$\eta^T \left( 1 - \frac{\dot{\sigma}_{LB}^Y}{\beta \dot{W}^Y} \right)^{-1} \leq \eta^X \leq \left( 1 + \frac{\dot{\sigma}_{LB}^X}{-\beta \dot{W}^X} \right)^{-1}. \quad (25)$$

In the context of Markovian dynamics, the recently derived bound [35] provides tighter lower bounds of the partial entropy production rates  $\dot{\sigma}^X$  and  $\dot{\sigma}^Y$  for the Markovian dynamics [also see Appendix. A]:

$$\begin{aligned} \dot{\sigma}^X &\geq \frac{(\dot{S}_r^X)^2}{\Theta^X}, \\ \dot{\sigma}^Y &\geq \frac{(\dot{S}_r^Y)^2}{\Theta^Y}, \end{aligned} \quad (26)$$

where

$$\Theta^X = \frac{1}{2} \sum_{x,x',y,v} \left( \ln \frac{W_{xx'|y}^v}{W_{x'x|y}^v} \right)^2 W_{xx'|y}^v p(x', y), \quad (27)$$

and

$$\Theta^Y = \frac{1}{2} \sum_{y,y',x,v} \left( \ln \frac{W_{yy'|x}^v}{W_{y'y|x}^v} \right)^2 W_{yy'|x}^v p(y', x). \quad (28)$$

The inequalities specified in Eq. (26) clearly articulate the dynamic behaviors within a system interacting with a thermal bath. When bath  $v$  triggers a transition from state  $(x', y)$  to  $(x, y)$ , according to Eq. (15), the energy absorbed by the system during this process is represented by the equation  $E(x, y) - E(x', y) = -k_B T_v \ln \frac{W_{xx'|y}^v}{W_{x'x|y}^v}$ . Here,  $E(x, y)$  denotes the energy of the state  $(x, y)$ ,  $k_B$  is the Boltzmann constant, and  $T_v$  represents the temperature of bath  $v$ . The transition probability coefficient,  $W_{xx'|y}^v p(x', y)$ , measures the rate at which transitions between these states occur. Additionally, the factor  $\Theta^{X/Y}$  can be understood as a dynamic activity factor, quantifying the level of active transitions influenced by the energy exchanges between the states and the bath. Inserting these bounds into Eqs. (25) and (24) gives

$$\eta^T \left[ 1 + \frac{(\dot{S}_r^X)^2}{-\Theta^X \dot{W}^X} \right] \leq \eta^Y \leq 1 - \frac{(\dot{S}_r^Y)^2}{\Theta^Y \dot{W}^Y},$$

$$\eta^T \left[ 1 - \frac{(\dot{S}_r^Y)^2}{\Theta^Y \dot{W}^Y} \right]^{-1} \leq \eta^X \leq \left[ 1 + \frac{(\dot{S}_r^X)^2}{-\Theta^X \dot{W}^X} \right]^{-1}. \quad (29)$$

These two inequalities encapsulate a thorough formulation of our principal results, providing a systematic method for establishing efficiency boundaries for subsystems in relation to their interactions with the environment and determining minimal rates of entropy production. Then we define  $\eta_L^Y = \eta^T \left[ 1 + \frac{(\dot{S}_r^X)^2}{-\Theta^X \dot{W}^X} \right]$ ,  $\eta_U^Y = 1 - \frac{(\dot{S}_r^Y)^2}{\Theta^Y \dot{W}^Y}$ ,  $\eta_L^X = \eta^T \left[ 1 - \frac{(\dot{S}_r^Y)^2}{\Theta^Y \dot{W}^Y} \right]^{-1}$  and  $\eta_U^X = \left[ 1 + \frac{(\dot{S}_r^X)^2}{-\Theta^X \dot{W}^X} \right]^{-1}$ . As noted, Eq. (29) in our work bears similarity to Eq. (18) from Ref. [15]. This is because we have employed the same procedure to determine the bound on the efficiency of the two subsystems. Specifically, this involves substituting the explicit expression for the lower bound of the entropy production rate. However, owing to the differing system descriptions used, we have employed distinct approaches to derive the lower bound of the entropy production rate. In Ref. [15],

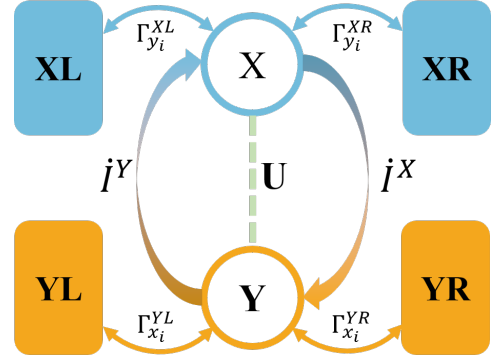


Figure 1. The schematic diagram of a double-quantum-dot system

the model is characterized by the overdamped Langevin equation, and the lower bound on the entropy production rate was derived using Jensen's inequality as detailed in [32]. Our findings are anchored within the framework of stochastic thermodynamics. For establishing the lower bound of the entropy production rate, we utilized the Cauchy-Schwarz inequality. Unlike Jensen's inequality, which necessitates convexity of the function, Cauchy-Schwarz inequality imposes no such restriction. This property renders Cauchy-Schwarz inequality more versatile within the context of stochastic thermodynamics.

### III. THE DOUBLE-QUANTUM-DOT SYSTEM

The double-quantum-dot (DQD) system consists of two quantum dots interacting via a Coulomb repulsion  $U$ . The DQD [See Fig. 1] is modeled by the Hamiltonian

$$H_S = \varepsilon_X d_X^\dagger d_X + \varepsilon_Y d_Y^\dagger d_Y + U d_X^\dagger d_X d_Y^\dagger d_Y, \quad (30)$$

where  $d_X^\dagger$  ( $d_X$ ) creates (annihilates) one electron on QD  $X$  with energy  $\varepsilon_X$ , and  $d_Y^\dagger$  ( $d_Y$ ) creates (annihilates) one electron on QD  $Y$  with energy  $\varepsilon_Y$ . QD  $X$  ( $Y$ ) is weakly coupled to two Fermi reservoirs  $XL$  and  $XR$  ( $YL$  and  $YR$ ). Thus, electrons are transported through parallel interacting channels. The Hamiltonian of the reservoirs is given by

$$H_B = \sum_k \sum_{\alpha \in \{X, Y\}} \sum_{\beta \in \{L, R\}} \varepsilon_{k\alpha\beta} c_{k\alpha\beta}^\dagger c_{k\alpha\beta}, \quad (31)$$

where  $c_{k\alpha\beta}^\dagger$  ( $c_{k\alpha\beta}$ ) is the creation (annihilation) operator at energy level  $\varepsilon_{k\alpha\beta}$  in bath  $\alpha\beta$ . The interaction between the DQD and the environment reads

$$H_I = \sum_k \sum_{\alpha \in \{X, Y\}} \sum_{\beta \in \{L, R\}} \left( t_{k\alpha\beta} d_\alpha c_{k\alpha\beta}^\dagger + t_{k\alpha\beta}^* c_{k\alpha\beta} d_\alpha^\dagger \right), \quad (32)$$

where  $t_{k\alpha\beta}$  denotes the coupling strength of the transition between QD  $\alpha$  and reservoir  $\alpha\beta$  at energy level  $\varepsilon_{k\alpha\beta}$ .

We use  $x_0$  and  $y_0$  ( $x_1$  and  $y_1$ ) to denote that  $X$  and  $Y$  are in empty (filled) states, respectively. The energy eigenstates of the DQD coincide with the localized Fock states  $|(x_0, y_0)\rangle$ ,  $|(x_1, y_0)\rangle$ ,  $|(x_0, y_1)\rangle$ , and  $|(x_1, y_1)\rangle$ , where their respective eigenvalues are  $0, \varepsilon_X, \varepsilon_Y$ , and  $\varepsilon_X + \varepsilon_Y + U$ .

For a non-degenerate system weakly coupled to different environmental modes, the dynamics of the populations satisfies Eq. (1). The transition rates follow from Fermi's golden rule and are given by

$$\begin{aligned} W_{x_1 x_0 | y_i}^v &= \Gamma_{y_i}^v f_{y_i}^v, \\ W_{x_0 x_1 | y_i}^v &= \Gamma_{y_i}^v (1 - f_{y_i}^v), \\ W_{y_1 y_0 | x_i}^v &= \Gamma_{x_i}^v f_{x_i}^v, \\ W_{y_0 y_1 | x_i}^v &= \Gamma_{x_i}^v (1 - f_{x_i}^v), \end{aligned}$$

where  $f_{x_i}^v = \{1 + \exp[\beta_v (\varepsilon_Y + iU - \mu_v)]\}^{-1}$  and  $f_{y_i}^v = \{1 + \exp[\beta_v (\varepsilon_X + iU - \mu_v)]\}^{-1}$  ( $i = 0, 1$ ) are the Fermi distribution functions,  $\beta_v = 1/(k_B T_v)$ , and  $\Gamma_{y_i}^v$  ( $\Gamma_{x_i}^v$ ) is a positive constant that characterizes the height of the potential barrier between  $X$  ( $Y$ ) and reservoir  $v$ . The potential barrier of  $Y$ , characterized by  $\Gamma_{x_i}^v$ , depends on the state of  $X$ , and vice versa. Note that  $\ln \frac{W_{x_1 x_0 | y_0}^v}{W_{x_0 x_1 | y_0}^v} = \beta_v (\varepsilon_X - \mu_v)$  and  $\ln \frac{W_{x_1 x_0 | y_1}^v}{W_{x_0 x_1 | y_1}^v} = \beta_v (\varepsilon_X + U - \mu_v)$ . Thus, for the quantum dot model, the parameter  $\Delta_{xx'}$  in Eq. (15) is equal to  $-\mu_v$  and will affect the heat flow.

For the purpose of reducing the number of parameters, the energy dependences of the tunneling rates are parametrized by dimensionless parameters  $\delta$  and  $\Delta$ , i.e.,

$$\begin{aligned} \Gamma_{x_0}^{YL} &= \Gamma \frac{e^\Delta}{\cosh(\Delta)}, & \Gamma_{x_1}^{YL} &= \Gamma \frac{e^{-\Delta}}{\cosh(\Delta)}, \\ \Gamma_{x_0}^{YR} &= \Gamma \frac{e^{-\Delta}}{\cosh(\Delta)}, & \Gamma_{x_1}^{YR} &= \Gamma \frac{e^\Delta}{\cosh(\Delta)}, \\ \Gamma_{y_0}^{XL} &= \Gamma \frac{e^\delta}{\cosh(\delta)}, & \Gamma_{y_1}^{XL} &= \Gamma \frac{e^{-\delta}}{\cosh(\delta)}, \\ \Gamma_{y_0}^{XR} &= \Gamma \frac{e^{-\delta}}{\cosh(\delta)}, & \Gamma_{y_1}^{XR} &= \Gamma \frac{e^\delta}{\cosh(\delta)}. \end{aligned} \quad (33)$$

The dimensionless parameters  $\delta$  and  $\Delta$  thus allow us to control the tunneling rates under different conditions. When  $\delta = \Delta = 0$ , this corresponds to the scenario of completely symmetric and equal tunneling rates. Conversely, in the limit where  $\delta$  approaches infinity, an electron in channel  $X$  can only enter and exit from reservoir  $XL$  at energy  $\varepsilon_X$ , whereas tunneling processes to reservoir  $XR$  are permitted at energy  $\varepsilon_X + U$ . In this limit, transport is possible only through energy exchange with channel  $Y$ . Similarly, the parameter  $\Delta$  controls the behavior of channel  $Y$ . According to Eqs. (7)-(10), (27), and (28), the entropy flows associated with subsystem  $X$  and  $Y$

$$\begin{aligned} \dot{S}_r^X &= -\beta \Delta \mu_X \left( J_{x_0 x_1 | y_0}^{XR} + J_{x_0 x_1 | y_1}^{XR} \right) \\ &\quad - \beta U \left( J_{y_1 y_0 | x_0}^{YL} + J_{y_1 y_0 | x_0}^{YR} \right), \end{aligned} \quad (34)$$

$$\begin{aligned} \dot{S}_r^Y &= -\beta \Delta \mu_Y \left( J_{y_0 y_1 | x_0}^{YR} + J_{y_0 y_1 | x_1}^{YR} \right) \\ &\quad - \beta U \left( J_{x_1 x_0 | y_0}^{XL} + J_{x_1 x_0 | y_0}^{XR} \right), \end{aligned} \quad (35)$$

the rate of informations

$$\dot{I}^X = \left( J_{y_1 y_0 | x_0}^{YL} + J_{y_1 y_0 | x_0}^{YR} \right) \ln \frac{p(x_0, y_1) p(x_1, y_0)}{p(x_0, y_0) p(x_1, y_1)}, \quad (36)$$

$$\dot{I}^Y = \left( J_{x_1 x_0 | y_0}^{XL} + J_{x_1 x_0 | y_0}^{XR} \right) \ln \frac{p(y_0, x_1) p(y_1, x_0)}{p(y_0, x_0) p(y_1, x_1)}, \quad (37)$$

and the coefficients

$$\begin{aligned} \Theta^X &= \frac{1}{2} (\varepsilon_X - \mu_{XL})^2 \left[ W_{10|0}^{XL} p(0, 0) + W_{01|0}^{XL} p(1, 0) \right] \\ &\quad + \frac{1}{2} (\varepsilon_X - \mu_{XR})^2 \left[ W_{10|0}^{XR} p(0, 0) + W_{01|0}^{XR} p(1, 0) \right] \\ &\quad + \frac{1}{2} (\varepsilon_X + U - \mu_{XL})^2 \left[ W_{10|1}^{XL} p(0, 1) + W_{01|1}^{XL} p(1, 1) \right] \\ &\quad + \frac{1}{2} (\varepsilon_X + U - \mu_{XR})^2 \left[ W_{10|1}^{XR} p(0, 1) + W_{01|1}^{XR} p(1, 1) \right], \end{aligned} \quad (38)$$

$$\begin{aligned} \Theta^Y &= \frac{1}{2} (\varepsilon_Y - \mu_{YL})^2 \left[ W_{10|0}^{YL} p(0, 0) + W_{01|0}^{YL} p(1, 0) \right] \\ &\quad + \frac{1}{2} (\varepsilon_Y - \mu_{YR})^2 \left[ W_{10|0}^{YR} p(0, 0) + W_{01|0}^{YR} p(1, 0) \right] \\ &\quad + \frac{1}{2} (\varepsilon_Y + U - \mu_{YL})^2 \left[ W_{10|1}^{YL} p(0, 1) + W_{01|1}^{YL} p(1, 1) \right] \\ &\quad + \frac{1}{2} (\varepsilon_Y + U - \mu_{YR})^2 \left[ W_{10|1}^{YR} p(0, 1) + W_{01|1}^{YR} p(1, 1) \right]. \end{aligned} \quad (39)$$

#### IV. RESULTS AND DISCUSSION

Figure 2 plots the efficiencies  $\eta^X$  and  $\eta^Y$ , upper bounds  $\eta_U^X$  and  $\eta_U^Y$ , and lower bounds  $\eta_L^X$  and  $\eta_L^Y$  for subsystems  $X$  and  $Y$  varying with the dimensionless Coulomb interaction strength  $\beta U$  and the parameter  $\delta$  and  $\Delta$  associated with the tunneling rate.

From Figure 2(a), it is evident that for subsystem  $X$ , the discrepancy between the upper bound  $\eta_U^X$  and the actual efficiency  $\eta^X$  is very minimal, and this difference decreases significantly as the value of  $\delta$  increases. Furthermore, when  $\delta$  is held constant, the lower bound  $\eta_L^X$  becomes progressively tighter as  $\beta U$  decreases. It is worth emphasizing that when both  $\beta U$  and  $\delta$  are small, the three efficiencies—upper bound, actual efficiency, and lower bound—converge closely to one another.

On the other hand, Figure 2(b) presents the results for subsystem  $Y$ . These results indicate that the upper bound  $\eta_U^Y$  becomes tighter primarily when  $\beta U$  is small.

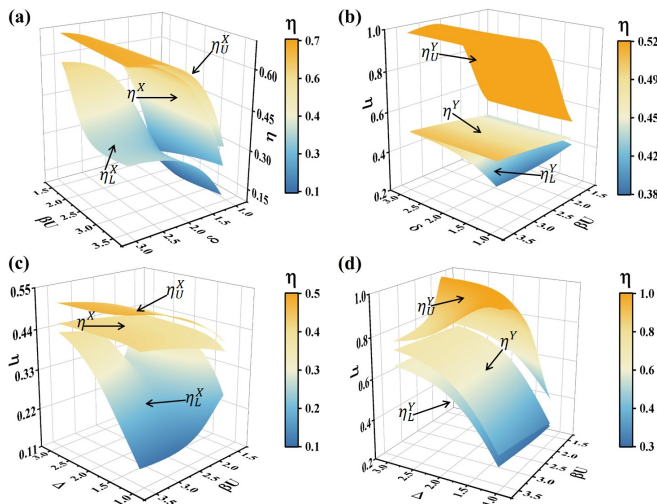


Figure 2. The efficiencies  $\eta^X$  and  $\eta^Y$ , upper bounds  $\eta_U^X$  and  $\eta_U^Y$ , and lower bounds  $\eta_L^X$  and  $\eta_L^Y$  for the double-quantum-dot system vary with the dimensionless Coulomb interaction strength  $\beta U$  and the parameters  $\delta$  and  $\Delta$  associated with the tunneling rate, where  $\beta(\mu_{XR} - \mu_{XL}) = 1$ ,  $\beta(\mu_{YR} - \mu_{YL}) = 2$ ,  $\Gamma = 1$ ,  $\varepsilon_X = \frac{(\mu_{XR} + \mu_{XL})}{2} - \frac{U}{2}$ , and  $\varepsilon_Y = \frac{(\mu_{YR} + \mu_{YL})}{2} - \frac{U}{2}$ . For (a) and (b), the variations are with  $\beta U$  and  $\delta$ , where  $\Delta = 1.5$ . For (c) and (d), the variations are with  $\beta U$  and  $\Delta$ , where  $\delta = 1.5$ .

As  $\beta U$  increases, this upper bound approaches the general result, namely  $\eta^Y \leq 1$ . Therefore, the discussion mainly pertains to the lower bound  $\eta_L^Y$ , which becomes very tight under low limits. When  $\beta U$  is fixed, a larger  $\delta$  improves the effectiveness of the lower bound as a limit. Similarly, when  $\delta$  is fixed, a larger lower limit of  $\beta U$  enhances the effectiveness of this boundary. When both  $\beta U$  and  $\delta$  are large, the lower bound is notably stringent. When we adjust  $\beta U$  and  $\Delta$ , the results are shown in Figures 2(c) and (d). It can be observed that the overall trend is consistent with the adjustments of  $\beta U$  and  $\delta$ . These show that our boundaries are reliable.

Additionally, it is important to note that in the definition of efficiency in Eq. (21), we assume  $\dot{W}^X \leq 0$  and  $\dot{W}^Y > 0$  for this model. Therefore, for the quantum dot model described in Sec. III, there exists a certain range of parameter values that enable the proper operation of

the bipartite system. For example, as shown in Figure 2(a), when both  $\beta U$  and  $\delta$  are small, the three efficiencies converge. This convergence occurs because a small value of  $\beta U$  indicates a very weak interaction between the two subsystems. Simultaneously, within the range of small values of  $\delta$ , the work  $\dot{W}^X$  tends to zero. This results in the bipartite system failing to operate normally. Consequently, all three efficiencies converge towards zero under these conditions.

## V. CONCLUSIONS

This paper successfully establishes a foundational lower bound on the entropy production rate of subsystems by employing the Cauchy-Schwarz inequality, leading to a significant advancement in understanding the efficiency boundaries of dual subsystems. The derivation of these efficiency bounds, grounded in the lower limit of entropy production, ensures applicability to both finely and coarsely-grained systems. Our empirical investigations, utilizing the double-quantum-dot system, not only validate the proposed inequalities but also demonstrate their capability to significantly tighten the efficiency boundaries. This work, deeply rooted in the principles of stochastic thermodynamics, offers invaluable insights applicable to a wide range of quantum-dot systems.

## ACKNOWLEDGMENTS

This work has been supported by the National Natural Science Foundation (Grants No. 12075197 and 12364008), Natural Science Foundation of Fujian Province (Grant No. 2023J01006), Fundamental Research Fund for the Central Universities (No. 20720240145), Guiding Project of Fujian Provincial Department of Science and Technology (2021H0051), and Talent Project of Quanzhou Science and Technology Bureau (2020C029R).

## Appendix A: Derivation of the bound of the entropy production rate of subsystem $X$

In this section, we provide a brief derivation of the efficiency limit for learning. Firstly, we evaluate the upper bound of  $\left| \dot{S}_r^X \right|$  as follows

$$\begin{aligned}
|\dot{S}_r^X| &= \left| \frac{1}{2} \sum_{x,x',y,v} J_{xx'|y}^v \ln \frac{W_{xx'|y}^v}{W_{x'x|y}^v} \right| \\
&= \left| \frac{1}{2} \sum_{x,x',y,v} \ln \frac{W_{xx'|y}^v}{W_{x'x|y}^v} \sqrt{W_{xx'|y}^v p(x',y) + W_{x'x|y}^v p(x,y)} \frac{J_{xx'|y}^v}{\sqrt{W_{xx'|y}^v p(x',y) + W_{x'x|y}^v p(x,y)}} \right| \\
&\stackrel{(1)}{\leq} \frac{1}{2} \sqrt{\sum_{x,x',y,v} \left( \ln \frac{W_{xx'|y}^v}{W_{x'x|y}^v} \right)^2 [W_{xx'|y}^v p(x',y) + W_{x'x|y}^v p(x,y)]} \sqrt{\sum_{x,x',y,v} \frac{(J_{xx'|y}^v)^2}{W_{xx'|y}^v p(x',y) + W_{x'x|y}^v p(x,y)}} \\
&\stackrel{(2)}{\leq} \frac{1}{2} \sqrt{\sum_{x,x',y,v} \left( \ln \frac{W_{xx'|y}^v}{W_{x'x|y}^v} \right)^2 [W_{xx'|y}^v p(x',y) + W_{x'x|y}^v p(x,y)]} \sqrt{\frac{1}{2} \sum_{x,x',y,v} J_{xx'|y}^v \ln \frac{W_{xx'|y}^v p(x',y)}{W_{x'x|y}^v p(x,y)}} \\
&= \frac{1}{2} \sqrt{\sum_{x,x',y,v} \left( \ln \frac{W_{xx'|y}^v}{W_{x'x|y}^v} \right)^2 [W_{xx'|y}^v p(x',y) + W_{x'x|y}^v p(x,y)]} \sqrt{\dot{\sigma}^X} \\
&= \sqrt{\frac{1}{2} \sum_{x,x',y,v} \left( \ln \frac{W_{xx'|y}^v}{W_{x'x|y}^v} \right)^2 W_{xx'|y}^v p(x',y)} \sqrt{\dot{\sigma}^X} \\
&= \sqrt{\Theta^X \dot{\sigma}^X}.
\end{aligned} \tag{A1}$$

This evaluation incorporates the Cauchy-Schwartz inequality [21, 22] and the inequality  $\frac{(x-y)^2}{x+y} \leq \frac{x-y}{2} \log \frac{x}{y}$  for nonnegative  $x$  and  $y$  in step (1) and (2), respectively. With the application of Eq. (A1), we naturally derive the lower limit on the entropy-production rate of subsystem  $X$ , as presented in Eq. (26) in the main text.

- 
- |   |  |
|---|--|
| <p>[1] U. Seifert, Reports on progress in physics <b>75</b>, 126001 (2012).</p> <p>[2] C. Van den Broeck and M. Esposito, Physica A: Statistical Mechanics and its Applications <b>418</b>, 6 (2015).</p> <p>[3] R. Landauer, IBM journal of research and development <b>5</b>, 183 (1961).</p> <p>[4] H. Dong, D. Xu, C. Cai, C. Sun, <i>et al.</i>, Physical Review E <b>83</b>, 061108 (2011).</p> <p>[5] A. Béruit, A. Arakelyan, A. Petrosyan, S. Ciliberto, R. Dillenschneider, and E. Lutz, Nature <b>483</b>, 187 (2012).</p> <p>[6] S. Dago, J. Pereda, N. Barros, S. Ciliberto, and L. Bellon, Physical Review Letters <b>126</b>, 170601 (2021).</p> <p>[7] K. Hashimoto and C. Uchiyama, Entropy <b>24</b>, 548 (2022).</p> <p>[8] T. Van Vu and K. Saito, Physical Review Letters <b>128</b>, 010602 (2022).</p> <p>[9] K. Proesmans, J. Ehrich, and J. Bechhoefer, Physical Review Letters <b>125</b>, 100602 (2020).</p> <p>[10] Y.-Z. Zhen, D. Egloff, K. Modi, and O. Dahlsten, Physical Review Letters <b>127</b>, 190602 (2021).</p> <p>[11] S. W. Kim, T. Sagawa, S. De Liberato, and M. Ueda, Physical Review Letters <b>106</b>, 070401 (2011).</p> <p>[12] J. V. Koski, V. F. Maisi, J. P. Pekola, and D. V. Averin, Proceedings of the National Academy of Sciences <b>111</b>, 13786 (2014).</p> <p>[13] P. Minalgaretti and H. Stark, Physical Review Letters <b>129</b>, 228005 (2022).</p> <p>[14] F. Chen, Y. Gao, and M. Galperin, Entropy <b>19</b>, 472 (2017).</p> | <p>[15] M. P. Leighton and D. A. Sivak, Physical Review Letters <b>130</b>, 178401 (2023).</p> <p>[16] A. C. Barato and U. Seifert, Physical Review Letters <b>114</b>, 158101 (2015).</p> <p>[17] J. M. Horowitz and T. R. Gingrich, Nature Physics <b>16</b>, 15 (2020).</p> <p>[18] N. Shiraishi, Journal of Statistical Physics <b>185</b>, 19 (2021).</p> <p>[19] N. Shiraishi, K. Saito, and H. Tasaki, Physical Review Letters <b>117</b>, 190601 (2016).</p> <p>[20] P. Pietzonka and U. Seifert, Physical Review Letters <b>120</b>, 190602 (2018).</p> <p>[21] K. Funo, N. Shiraishi, and K. Saito, New Journal of Physics <b>21</b>, 013006 (2019).</p> <p>[22] N. Shiraishi, K. Funo, and K. Saito, Physical Review Letters <b>121</b>, 070601 (2018).</p> <p>[23] T. Van Vu and Y. Hasegawa, Physical Review Letters <b>126</b>, 010601 (2021).</p> <p>[24] E. Aurell, C. Mejía-Monasterio, and P. Muratore-Ginanneschi, Physical Review Letters <b>106</b>, 250601 (2011).</p> <p>[25] T. Van Vu and Y. Hasegawa, Physical Review Letters <b>127</b>, 190601 (2021).</p> <p>[26] H. Tajima and K. Funo, Physical Review Letters <b>127</b>, 190604 (2021).</p> <p>[27] G. E. Crooks, Physical Review Letters <b>99</b>, 100602 (2007).</p> <p>[28] P. Salamon and R. S. Berry, Physical Review Letters <b>51</b>, 1127 (1983).</p> |
|---|--|

- [29] D. A. Sivak and G. E. Crooks, *Physical Review Letters* **108**, 190602 (2012).
- [30] M. Scandi and M. Perarnau-Llobet, *Quantum* **3**, 197 (2019).
- [31] J.-F. Chen, C. Sun, and H. Dong, *Physical Review E* **104**, 034117 (2021).
- [32] M. P. Leighton and D. A. Sivak, *Physical Review Letters* **129**, 118102 (2022).
- [33] T. Tanogami, T. Van Vu, and K. Saito, *Physical Review Research* **5**, 043280 (2023).
- [34] J. M. Horowitz and M. Esposito, *Physical Review X* **4**, 031015 (2014).
- [35] S. Su, J. Chen, Y. Wang, J. Chen, and C. Uchiyama, arXiv preprint arXiv:2209.08096 (2022).
- [36] L. Peliti and S. Pigolotti, *Stochastic thermodynamics: an introduction* (Princeton University Press, 2021).